

The $ep \rightarrow e'p\eta$ reaction at and above the $S_{11}(1535)$ baryon resonance

R. Thompson,¹ S. Dytman,¹ K.Y. Kim,¹ J. Mueller,¹ G.S. Adams,²² M.J. Amarian,³⁵ E. Anciant,²⁴ M. Anghinolfi,¹³ B. Asavapibhop,²⁸ T. Auger,²⁴ G. Audit,²⁴ H. Avakian,¹² S. Barrow,¹⁰ M. Battaglieri,¹³ K. Beard,¹⁶ M. Bektasoglu,²¹ B.L. Berman,¹¹ W. Bertozzi,¹⁸ N. Bianchi,¹² A. Biselli,²² S. Boiarinov,¹⁴ B.E. Bonner,²³ W.J. Briscoe,¹¹ W. Brooks,²⁵ V.D. Burkert,²⁵ J.R. Calarco,²⁹ G. Capitani,¹² D.S. Carman,²⁰ B. Carnahan,⁴ C. Cetina,¹¹ P.L. Cole,³² A. Coleman,⁶ J. Connelly,¹¹ D. Cords,²⁵ P. Corvisiero,¹³ D. Crabb,³³ H. Crannell,⁴ J. Cummings,²² D. Day,³³ P.V. Degtyarenko,²⁵ R.A. Demirchyan,³⁵ L.C. Dennis,¹⁰ A. Deppman,¹² E. De Sanctis,¹² R. De Vita,¹³ K.S. Dhuga,¹¹ C. Djalali,³¹ G.E. Dodge,²¹ D. Doughty,^{5 25} P. Dragovitsch,¹⁰ M. Dugger,² M. Eckhause,⁶ Y.V. Efremenko,¹⁴ H. Egiyan,⁶ K.S. Egiyan,³⁵ L. Elouadrhiri,^{5 25} L. Farhi,²⁴ R.J. Feuerbach,³ J. Ficenec,³⁴ K. Fissum,¹⁸ A. Freyberger,²⁵ H. Funsten,⁶ M. Gai,²⁷ V.B. Gavrilo, ¹⁴ G.P. Gilfoyle,³⁰ K. Giovanetti,¹⁶ S. Gilad,¹⁸ P. Girard,³¹ K.A. Griffioen,⁶ M. Guidal,¹⁵ M. Guillo,³¹ V. Gyurjyan,²⁵ D. Hancock,⁶ J. Hardie,^{5 25} D. Heddle,^{5 25} J. Heisenberg,²⁹ F.W. Hersman,²⁹ K. Hicks,²⁰ R.S. Hicks,²⁸ M. Holtrop,²⁹ C.E. Hyde-Wright,²¹ M.M. Ito,²⁵ D. Jenkins,³⁴ K. Joo,³³ J. Kane,⁶ M. Khandaker,^{19 25} W. Kim,¹⁷ A. Klein,²¹ F.J. Klein,^{9 25} M. Klusman,²² M. Kossov,¹⁴ S.E. Kuhn,²¹ Y. Kuang,⁶ J.M. Laget,²⁴ D. Lawrence,²⁸ G.A. Leskin,¹⁴ A. Longhi,⁴ K. Loukachine,³⁴ M. Lucas,³¹ R. Magahiz,³ R.W. Major,³⁰ J.J. Manak,²⁵ C. Marchand,²⁴ S.K. Matthews,⁴ L. Maximon,¹¹ S. McAleer,¹⁰ J. McCarthy,³³ J.W.C. McNabb,³ B.A. Mecking,²⁵ M.D. Mestayer,²⁵ C.A. Meyer,³ R. Minehart,³³ M. Mirazita,¹² R. Miskimen,²⁸ V. Muccifora,¹² L. Murphy,¹¹ G.S. Mutchler,²³ J. Napolitano,²² R.A. Niyazov,²¹ M.S. Ohandjanyan,³⁵ J.T. O'Brien,⁴ A. Opper,²⁰ Y. Patois,³¹ F. Perrot-Kunne,²⁴ G.A. Peterson,²⁸ S. Philips,¹¹ N. Pivnyuk,¹⁴ D. Pocanic,³³ O. Pogorelko,¹⁴ E. Polli,¹² B.M. Preedom,³¹ J.W. Price,²⁶ L.M. Qin,²¹ B.A. Raue,^{9 25} A.R. Reolon,¹² G. Riccardi,¹⁰ G. Ricco,¹³ M. Ripani,¹³ B.G. Ritchie,² F. Ronchetti,¹² P. Rossi,¹² F. Roudot,²⁴ D. Rowntree,¹⁸ P.D. Rubin,³⁰ C.W. Salgado,^{19 25} M. Sanzone,¹² V. Sapunenko,¹³ A. Sarty,¹⁰ M. Sargsyan,³⁵ R.A. Schumacher,³ A. Shafi,¹¹ Y.G. Sharabian,³⁵ J. Shaw,²⁸ S.M. Shuvalov,¹⁴ A. Skabelin,¹⁸ T. Smith,²⁹ C. Smith,³³ E.S. Smith,²⁵ D.I. Sober,⁴ M. Spraker,⁷ S. Stepanyan,³⁵ P. Stoler,²² M. Taiuti,¹³ M.F. Taragin,¹¹ S. Taylor,²³ D. Tedeschi,³¹ T.Y. Tung,⁶ M.F. Vineyard,³⁰ A. Vlassov,¹⁴ H. Weller,⁷ L.B. Weinstein,²¹ R. Welsh,⁶ D.P. Weygand,²⁵ S. Whisnant,³¹ M. Witkowski,²² E. Wolin,²⁵ A. Yegneswaran,²⁵ J. Yun,²¹ Z. Zhou,¹⁸ J. Zhao¹⁸

(The CLAS Collaboration)

¹University of Pittsburgh, Department of Physics and Astronomy, Pittsburgh, PA 15260, USA

²Arizona State University, Department of Physics and Astronomy, Tempe, AZ 85287, USA

³Carnegie Mellon University, Department of Physics, Pittsburgh, PA 15213, USA

⁴Catholic University of America, Department of Physics, Washington D.C., 20064, USA

⁵Christopher Newport University, Newport News, VA 23606, USA

⁶College of William and Mary, Department of Physics, Williamsburg, VA 23187, USA

⁷Duke University, Physics Bldg. TUNL, Durham, NC27706, USA

⁸Department of Physics and Astronomy, Edinburgh University, Edinburgh EH9 3JZ, United Kingdom

- ⁹ *Florida International University, Miami, FL 33199, USA*
- ¹⁰ *Florida State University, Department of Physics, Tallahassee, FL 32306, USA*
- ¹¹ *George Washington University, Department of Physics, Washington D. C., 20052 USA*
- ¹² *Istituto Nazionale di Fisica Nucleare, Laboratori Nazionali di Frascati, P.O. 13, 00044 Frascati, Italy*
- ¹³ *Istituto Nazionale di Fisica Nucleare, Sezione di Genova e Dipartimento di Fisica dell'Universita, 16146 Genova, Italy*
- ¹⁴ *Institute of Theoretical and Experimental Physics, 25 B. Cheremushkinskaya, Moscow, 117259, Russia*
- ¹⁵ *Institut de Physique Nucleaire d'Orsay, IN2P3, BP 1, 91406 Orsay, France*
- ¹⁶ *James Madison University, Department of Physics, Harrisonburg, VA 22807, USA*
- ¹⁷ *Kyungpook National University, Department of Physics, Taegu 702-701, South Korea*
- ¹⁸ *M.I.T.-Bates Linear Accelerator, Middleton, MA 01949, USA*
- ¹⁹ *Norfolk State University, Norfolk VA 23504, USA*
- ²⁰ *Ohio University, Department of Physics, Athens, OH 45701, USA*
- ²¹ *Old Dominion University, Department of Physics, Norfolk VA 23529, USA*
- ²² *Rensselaer Polytechnic Institute, Department of Physics, Troy, NY 12181, USA*
- ²³ *Rice University, Bonner Lab, Box 1892, Houston, TX 77251*
- ²⁴ *CEA Saclay, DAPNIA-SPhN, F91191 Gif-sur-Yvette Cedex, France*
- ²⁵ *Thomas Jefferson National Accelerator Facility, 12000 Jefferson Avenue, Newport News, VA 23606, USA*
- ²⁶ *University of California at Los Angeles, Department of Physics and Astronomy, Los Angeles, CA 90095-1547, USA*
- ²⁷ *University of Connecticut, Physics Department, Storrs, CT 06269, USA*
- ²⁸ *University of Massachusetts, Department of Physics, Amherst, MA 01003, USA*
- ²⁹ *University of New Hampshire, Department of Physics, Durham, NH 03824, USA*
- ³⁰ *University of Richmond, Department of Physics, Richmond, VA 23173, USA*
- ³¹ *University of South Carolina, Department of Physics, Columbia, SC 29208, USA*
- ³² *University of Texas at El Paso, Department of Physics, El Paso, Texas 79968, USA*
- ³³ *University of Virginia, Department of Physics, Charlottesville, VA 22903, USA*
- ³⁴ *Virginia Polytechnic and State University, Department of Physics, Blacksburg, VA 24061, USA*
- ³⁵ *Yerevan Physics Institute, 375036 Yerevan, Armenia*

(November 13, 2018)

Abstract

New cross sections for the reaction $ep \rightarrow ep\eta$ are reported for total center of mass energy $W=1.5\text{--}1.86$ GeV and invariant momentum transfer $Q^2=0.25\text{--}1.5$ (GeV/c)². This large kinematic range allows extraction of important new information about response functions, photocouplings, and ηN coupling strengths of baryon resonances. Expanded W coverage shows sharp structure at $W \sim 1.7$ GeV; this is shown to come from interference between S and P waves and can be interpreted in terms of known resonances. Improved values are derived for the photon coupling amplitude for the $S_{11}(1535)$ resonance.

PACS : 13.30.Eg, 13.60.Le, 14.20.Gk

The study of baryon resonances is undergoing a significant rebirth because of new experimental programs at Brookhaven, the Mainz microtron, the Bonn synchrotron, and Jefferson Lab. Continuous, polarized beams and large acceptance detectors are significantly improving experimental accuracy. Older studies found a few dozen states with a variety of total angular momentum, parity, and strangeness [1]. Modern theoretical work examines the microscopic structure in terms of quark and gluon interactions. Empirical constituent quark models (CQM) achieve excellent qualitative agreement with a variety of data [2] and provide important evidence that quark excitations in these states are more important than gluonic excitations. Lattice gauge models simulate full QCD; they presently calculate moderately accurate values for excited state masses [3] and show great promise. These studies require data of much higher quality than was previously available.

Disentangling the wide and overlapping states that populate reaction data is an historical problem. However, reactions involving ηN final states couple only to isospin $\frac{1}{2}$ resonances. Although πN elastic scattering close to ηN threshold (total c.m. energy, $W=1.485$ GeV) shows no strong signal of a resonance, a prominent peak in the total cross section is seen for η production in γN and πN experiments. This is widely interpreted as the excitation of a *single* resonance, the spin $\frac{1}{2}$, negative parity, isospin $\frac{1}{2}$ state $S_{11}(1535)$ [1]. (S labels the ηN orbital angular momentum.) This state has a branching ratio to ηN of 30-55% compared to a few percent [1,4] for other states. These unusual features have encouraged alternative theoretical efforts to describe the data in terms of a strong (possibly nonresonant) final state interaction [5].

Most previous experiments used pion beams. An important advantage of electromagnetic experiments is the ability to extract the matrix elements for $\gamma N \rightarrow N^*$, commonly called the photon coupling amplitudes. These amplitudes are primarily sensitive to the quark wave function used. They are labeled by the γN total helicity and the virtual photon polarization and depend on the invariant momentum transfer to the resonance (Q^2). For a spin $\frac{1}{2}$ resonance, there is one transverse amplitude ($A_{\frac{1}{2}}$) and one longitudinal amplitude ($S_{\frac{1}{2}}$).

Photoproduction experiments ($Q^2=0$) have reaffirmed the strong energy dependence and S -wave (isotropic) character close to threshold [6]. A recent experiment with polarized photons [7] has given new values for ηN decay branching ratios of other resonances through interference with the dominant $S_{11}(1535)$.

In electroproduction experiments, Q^2 is nonzero and provides additional structure information about the intermediate state. Past η electroproduction experiments [8–11] found an unusually flat Q^2 dependence of $A_{\frac{1}{2}}$ for the $S_{11}(1535)$ in contrast to the nucleon form factors and photon coupling amplitudes of other established resonances, e.g. $P_{33}(1232)$. At this time, there is no definitive explanation for this difference. Although previous angular distributions were largely isotropic at all Q^2 , no detailed response functions were extracted because of the poor angular coverage in traditional magnetic spectrometers. Here, η electroproduction is used to study the $S_{11}(1535)$ over a broad range of Q^2 and W . At higher W new interference effects are found that add to our knowledge of ηN coupling to higher mass resonances.

The results reported here used the CEBAF Large Acceptance Spectrometer (CLAS) at Jefferson Lab (JLab). It has moderate momentum resolution and excellent solid angle coverage for final state particles produced in collisions of photon or electron beams of up to

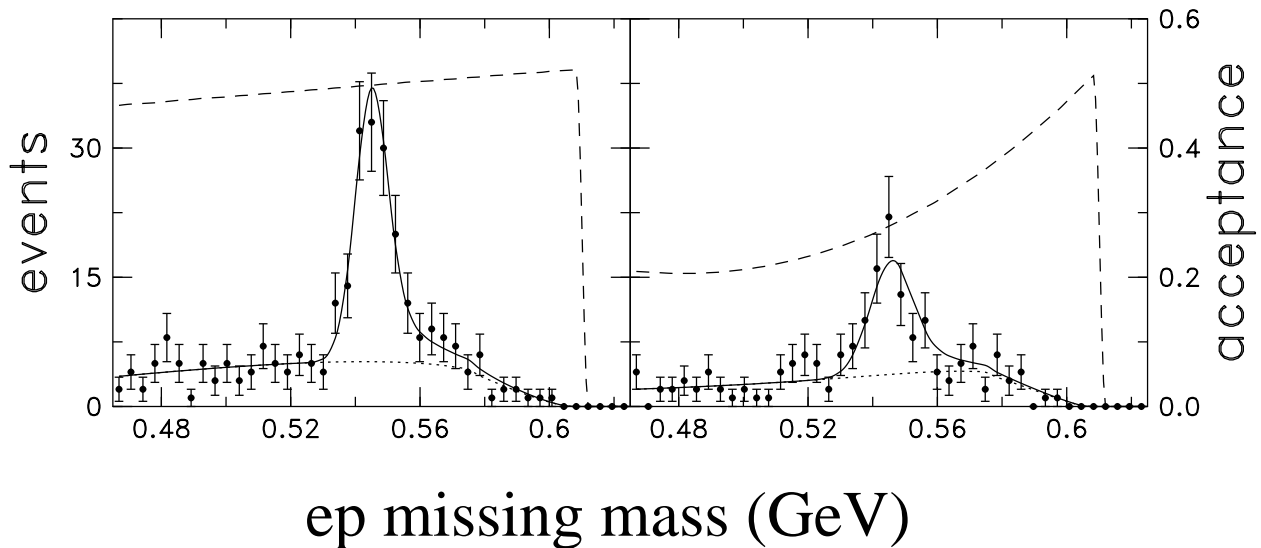


FIG. 1. Missing mass spectra for $ep \rightarrow epX$. Bins shown are for $W=1.535$ GeV and $Q^2=1.25$ $(\text{GeV}/c)^2$. Left plot is for $\phi_\eta^*=22.5^\circ$ and $\cos\theta_\eta^*=-0.4$; right plot is for $\phi_\eta^*=67.5^\circ$ and $\cos\theta_\eta^*=0.0$. The dashed line (right scale) shows the acceptance. The solid and dotted lines are the full fit function and the background function only.

5.5 GeV energy with various targets. This is advantageous for N^* experiments because the resonances decay to multiple particles spread over a large kinematic range.

The CLAS detector [12] measures angles and momenta of charged particles for lab polar angles (θ) in the range of 8-142°. For this measurement, electron beams with energies of 1.645 GeV ($0.25 < Q^2 < 0.5$ $(\text{GeV}/c)^2$) and 2.445 GeV ($0.5 < Q^2 < 1.5$ $(\text{GeV}/c)^2$) were incident on a liquid hydrogen target. A full description of these results can be found in Ref. [13]. An electron and proton were identified in the final state. The hardware trigger identified electrons through threshold Cerenkov detectors and an electromagnetic calorimeter. The proton was identified using the time-of-flight technique. Fiducial cuts were used to restrict particles to detector locations where the single particle detection efficiency is flat. Events for the angular distributions were binned in Q^2 , W , and the c.m. decay angles $\cos\theta_\eta^*$ and ϕ_η^* . For the angle integrated cross sections, the same events were binned in Q^2 and W .

η mesons were identified by fitting the missing mass spectrum (see Fig. 1). The fit function is the sum of a peak with a radiative tail and a background function. The background is due to multi-pion production reactions. Lacking a detailed understanding of the background, a simple function incorporating the proper behavior at the kinematic limit and the CLAS acceptance was used. Acceptance was calculated using a GEANT-based Monte Carlo simulation of the CLAS detector that included bremsstrahlung radiation using the peaking approximation. The maximum acceptance of these data is 54% and no cross section is reported where the acceptance was less than 5%.

A detailed study of potential sources of systematic error was made. The ep elastic cross section was determined from the same data set used for the new results. Agreement within about 5% of previous values was obtained, verifying the efficiency of the hardware trigger to the same level. Other studies estimated errors due to inexact knowledge of the peak shape and background, residual misalignment of the detectors, dependence of the acceptance on the Monte Carlo input distribution, and variations of the fiducial cut edges for the e and p .

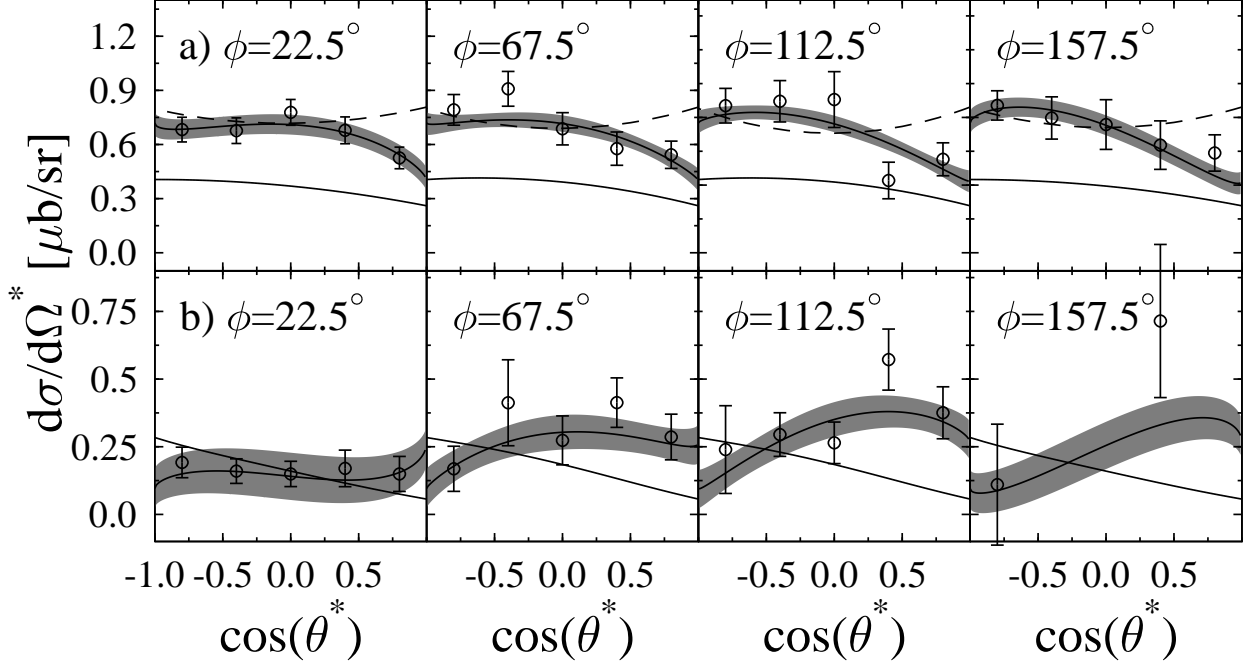


FIG. 2. Differential cross section for $\gamma_\nu p \rightarrow p\eta$ in the center of mass frame for a) $W=1.53$ GeV and $Q^2=1.25$ $(\text{GeV}/c)^2$ and b) $W=1.71$ GeV and $Q^2=0.75$ $(\text{GeV}/c)^2$. Values for ϕ_η^* symmetric about 180° have been averaged. (No information is lost this way; see Eq. (1).) Solid lines with an error band correspond to the response function fit described in the text. Dashed (solid) lines correspond to the effective Lagrangian calculation of the RPI (Mainz) group. See text for details.

The values varied between 0 and 10%. The total angle-dependent systematic error for each bin was the sum of all the components added in quadrature. Finally, the total error quoted was obtained by adding the error in the η yield, the acceptance error, and the systematic error in quadrature.

Angular distributions were measured as a function of c.m. decay angles $\cos\theta_\eta^*$ and ϕ_η^* for W for central bin values from 1.5 to 1.83 GeV and for $Q^2=0.375, 0.75$ and 1.25 $(\text{GeV}/c)^2$. Sample results for the virtual photon cross section in the center of mass frame are shown in Fig. 2. Although all distributions have a significant isotropic component, deviations from isotropy are seen.

Fig. 2 also shows predictions by the Mainz [14] and RPI [15] groups. Both models use effective Lagrangians with resonant and nonresonant terms. RPI fits parameters to photoproduction and high Q^2 data [11]. Their results are fairly consistent with the new data at low W but have the wrong slope at 1.62 GeV, perhaps due to problems with the u-channel. The Mainz model fits photoproduction data and extends to finite Q^2 using a CQM. They match the new data better at high W than RPI, but have the wrong magnitude at low W .

The exact virtual photon cross section is

$$\frac{d^2\sigma}{d\Omega_\eta^*} = \frac{|p_\eta^*|}{K_{cm}} \left[R_T + \epsilon R_L + R_{LT} \cdot \sqrt{\frac{\epsilon}{2}(\epsilon+1)} \cos\phi_\eta^* + R_{TT} \cdot \epsilon \cos 2\phi_\eta^* \right]. \quad (1)$$

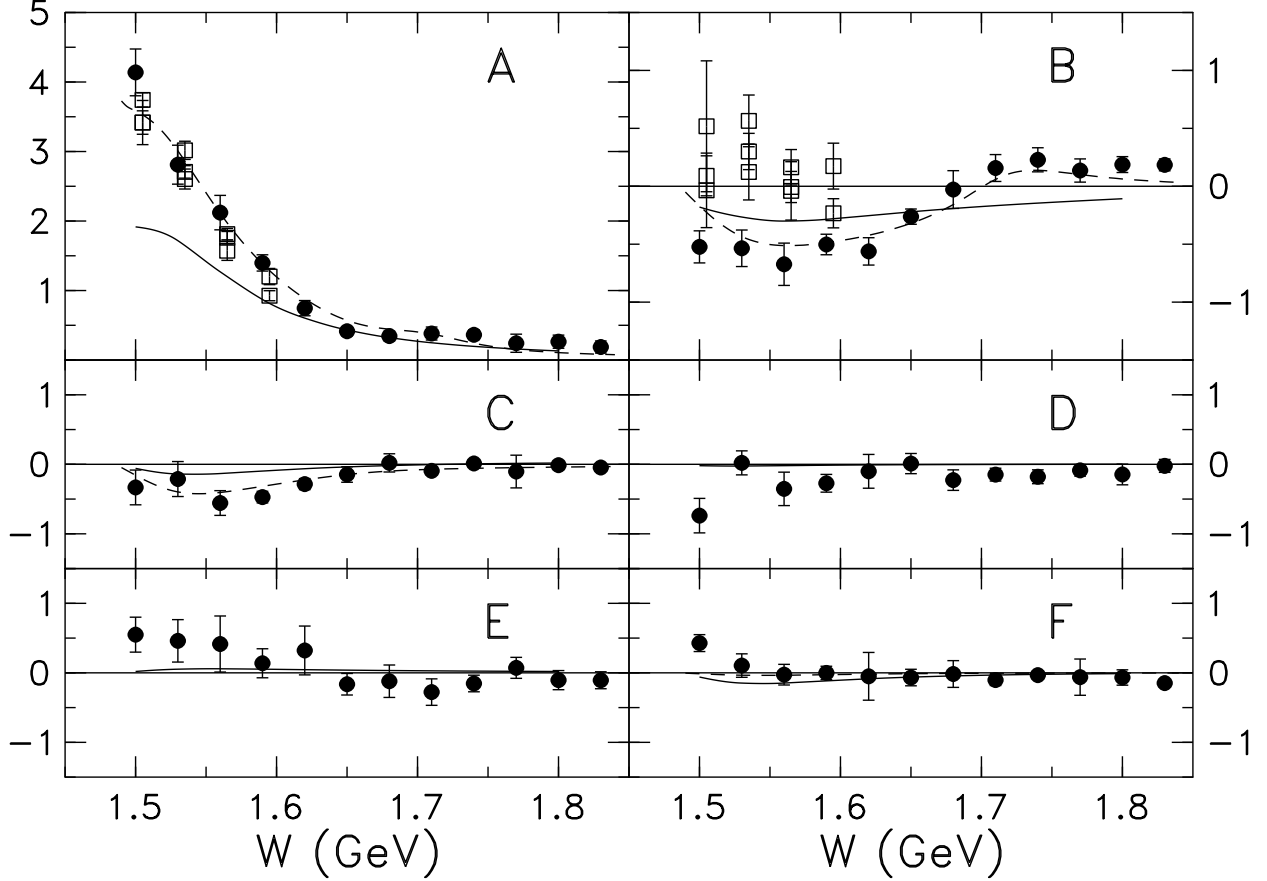


FIG. 3. Results of fitting the $Q^2=0.75$ (GeV/c) 2 angular distribution data of this experiment to Eq. (2). See text for details. Open squares are previous data [8]. Contributions from both statistical and systematic sources are displayed. The solid line is the theoretical prediction of the Mainz group and the dashed line is a five resonance fit to A, B, C, and F.

The angular distributions were fit to a form,

$$\begin{aligned}
&\approx \frac{|p_\eta^*|}{K_{cm}} \left[A + B \cdot \cos \theta_\eta^* + C \cdot P_2(\cos \theta_\eta^*) \right. \\
&\quad \left. + (D \cdot \sin \theta_\eta^* + E \cdot \sin \theta_\eta^* \cdot \cos \theta_\eta^*) \cdot \cos \phi_\eta^* \right. \\
&\quad \left. + F \cdot \sin^2 \theta_\eta^* \cdot \cos 2\phi_\eta^* \right], \quad (2)
\end{aligned}$$

assuming dominance of the S_{11} partial wave and truncation to total angular momentum up to $\frac{3}{2}$ [14]. Here ϵ is the polarization parameter and K_{cm} is the equivalent c.m. photon momentum. The parameters A , B , and C contain contributions from the longitudinal (R_L) and transverse (R_T) response functions, D and E parameterize the longitudinal-transverse interference response function (R_{LT}), and F contains the transverse-transverse interference response function (R_{TT}). Krusche et al. [6] used a similar form for photoproduction data, but only R_T contributes there. Fit results for $Q^2=0.75$ (GeV/c) 2 are shown in Fig. 3 along with the Mainz predictions [14].

Because of their limited kinematic ranges, previous experiments fit A and B [8] or A only [9–11]. A is mostly due to $S_{11}(1535)$ and is the largest amplitude. It is probably dominated by the transverse amplitude because the longitudinal contribution is known to

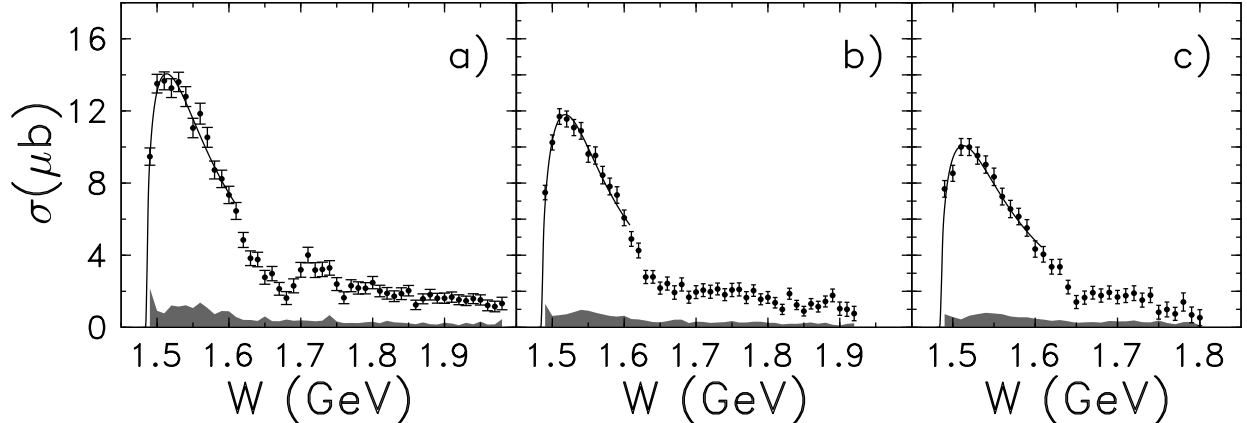


FIG. 4. New integrated cross section data at (a) $Q^2=0.625$ (GeV/c)², b) $Q^2=0.875$ (GeV/c)², and c) $Q^2=1.125$ (GeV/c)². The shaded band shows systematic errors. The curves correspond to single-resonance Breit-Wigner fits with an energy-dependent width over the energy range shown.

be minor [10]. The W dependence of both A and C are similar to what was seen in Krusche et al. [6].

Nonzero values for parameters $B - F$ are evidence for interference with overlapping resonances or nonresonant mechanisms. For the assumptions made, B and D come from interference between S_{11} and P_{11} partial waves, and C , E , and F come from interference between S_{11} and D_{13} partial waves. More complete partial wave analyses will be required to disentangle these contributions in detail.

Limitations in W for previous data are most evident in B . The value for electroproduction data [8] was positive and poorly determined. In the photoproduction experiment, B was slightly negative. The new result extends to much higher W . The sign change in B at $W \sim 1.7$ GeV has not been seen before. Such a rapid change is likely due to resonance effects, perhaps the onset of $P_{11}(1710)$. In fact, the W dependence of A , B , C , and F can be reproduced (see Fig. 3) in a simple isobar model by including $S_{11}(1535)$, $S_{11}(1650)$, $D_{13}(1520)$, $P_{11}(1440)$, and $P_{11}(1710)$ states with standard masses and widths [1]. Neither calculation in Fig. 2 includes the $P_{11}(1710)$.

R_{LT} and R_{TT} are small compared to the dominant transverse amplitude. D , E , and F are consistent with zero over almost all of the range of Q^2 and W covered. The Mainz predictions for these amplitudes are small. Due to a lack of statistics, the present data provide only a qualitative test of the predictions.

Angle integrated cross sections were also obtained for events in a given Q^2 , W bin using the same methods as for the angular distributions. Distributions in W for three Q^2 values are shown in Fig. 4. Structure is seen at $W \sim 1.7$ GeV. A dip followed by a peak is seen at $Q^2=0.625$ (GeV/c)² while a significant change in slope is seen at other Q^2 . This W is where B (see above) changes sign and both probably have the same cause.

Fits to a single Breit-Wigner ($S_{11}(1535)$ only) shape [14] are also shown in Fig. 4. The nonresonant contribution is ignored in this fit [14,15]. Results are very dependent on the W range chosen because other contributions become prominent at higher W . We find the best fit with a maximum W of 1.62 GeV. These fits give a resonance mass of 1522 ± 11 MeV and full width of 143 ± 18 MeV. A coupled-channels analysis will be required to get the most reliable values. The maximum cross section for the new and all previous experiments was

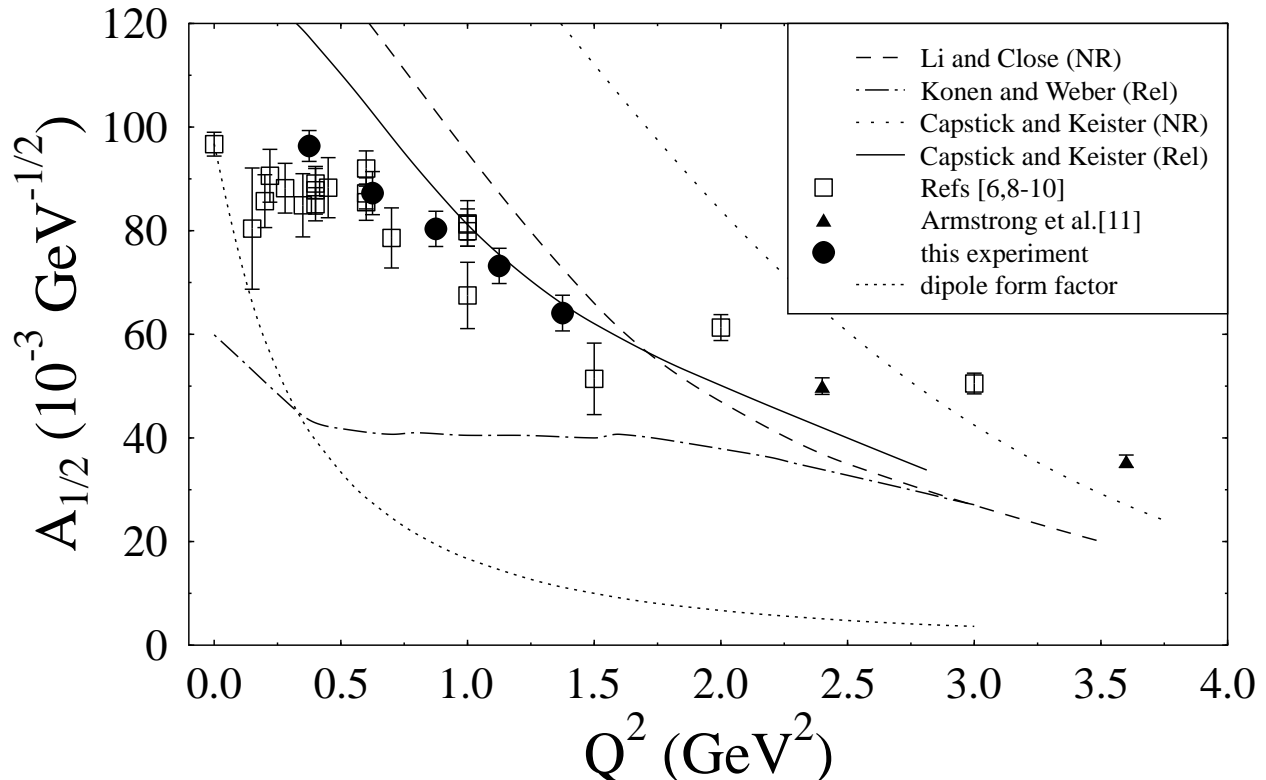


FIG. 5. Values of the photon coupling amplitude, $A_{1/2}$, for $\gamma p \rightarrow S_{11}(1535)$ obtained from the integrated cross section data of this experiment compared to previous data and various CQM calculations[16]. All statistical and systematic errors from data are included.

then used to determine $A_{\frac{1}{2}}$. For consistent comparison, a full width of 150 MeV and an $S_{11} \rightarrow \eta N$ branching fraction of 0.55 [4,11] were used. New and re-analyzed old measurements of $A_{\frac{1}{2}}$ are shown in Fig. 5. A number of values for $A_{\frac{1}{2}}$ from π and η photoproduction ($Q^2=0$) data with significant model dependence have been reported. The PDG value [1] of $0.09 \pm 0.03 \text{ GeV}^{-\frac{1}{2}}$ reflects this uncertainty. The theoretical calculations shown in Fig. 5 are nonrelativistic and relativistic CQM predictions [16]. None agrees well with the data or each other, an important failure of the CQM.

These and other recent data from JLab [11] have comparable values for the S_{11} Breit-Wigner width ($\sim 150 \text{ MeV}$) for Q^2 between 0.375 and 3.6 $(\text{GeV}/c)^2$. Photoproduction [6] and Brasse electroproduction values [8] are surprisingly different, 239 and $\sim 90 \text{ MeV}$, respectively, in our fits. At high Q^2 , the Brasse data is incompatible with Armstrong [11]; at low Q^2 , either the single resonance interpretation is incorrect or there is a significant change in dynamics with increasing Q^2 .

The eta electroproduction data shown here comprise one of the first results of the CLAS. It covers the region in W at and above the $S_{11}(1535)$ resonance in great detail. A consistent picture of the reaction is given over a more extensive kinematic range than any previous data. The values for the interference response functions are small compared to the dominant transverse response function and in qualitative agreement with theoretical predictions [14]. B measures the interference between S_{11} and P_{11} partial waves. It is more negative than the photoproduction results [6] at low W and changes sign at $W \sim 1.7 \text{ GeV}$, likely signalling

the onset of a strong P -wave process. At the same W , a sharp change in slope is seen in the integrated data. The angular distribution data can be described by a simple isobar model using known states. The ηN coupling strengths for these states are poorly known, but can be determined using these data. A simple determination of the $\gamma p \rightarrow S_{11}(1535)$ photon coupling amplitude provides new and far more consistent evidence for its unusually slow falloff with increasing Q^2 . These data along with other recent Jefferson Lab data [11] provide inescapable constraints on models attempting to describe the structure of $S_{11}(1535)$.

We acknowledge the efforts of the staff of the Accelerator and the Physics Divisions at JLab that made this experiment possible. This work was supported in part by the U.S. Department of Energy and National Science Foundation, the French Commissariat à l'Énergie Atomique, the Italian Istituto Nazionale di Fisica Nucleare, and the Korea Science and Engineering Foundation.

REFERENCES

- [1] D.E. Groom, et al., Eur. Phys. J. **C15**, 1 (2000).
- [2] S. Capstick, Phys. Rev. **D46**, 2864 (1992).
- [3] D.B. Leinweber, et al., Phys. Rev. **D61**:074502 (2000); S. Sasaki, hep-ph/0004252.
- [4] T.P. Vrana, S.A. Dytman, and T.-S. H. Lee, Phys. Repts. **328**, 181 (2000).
- [5] N. Kaiser, T. Waas and W. Weise, Nucl. Phys. **A612**, 297 (1997).
- [6] B. Krusche et al., Phys. Rev. Lett. **74**, 3736 (1995).
- [7] J. Ajaka et al., Phys. Rev. Lett. **81**, 1797 (1998).
- [8] F. W. Brasse et al., Nucl. Phys. **B139**, 37 (1978); F. W. Brasse et al., Z. Phys. **C22**, 33 (1984).
- [9] U. Beck et al., Phys. Lett. **B51**, 103 (1974).
- [10] H. Breuker et al., Phys. Lett. **B74**, 409 (1978).
- [11] C. S. Armstrong et al., Phys. Rev. **D60**:052004 (1999).
- [12] W. Brooks, Nucl. Phys. **A663-664**, 1077 (2000).
- [13] Richard A. Thompson, Ph. D. Thesis, University of Pittsburgh (unpublished), 2000.
- [14] G. Knochlein, D. Drechsel and L. Tiator, Z. Phys. **A352**, 327 (1995); L. Tiator, C. Bennhold, and S.S. Kamalov, Nucl. Phys. **A580**, 455 (1994).
- [15] M. Benmerrouche, N.C. Mukhopadhyay, and J.F. Zhang, Phys. Rev. **D51**, 3237 (1995); R. Davidson, priv. comm.
- [16] S. Capstick and B.D. Keister, Phys. Rev. **D51**, 3598 (1995); W. Konen and H.J. Weber, Phys. Rev. **D41**, 2241 (1990); F.E. Close and Z. Li, Phys. Rev. **D42**, 2194 (1990) .